

Radiation-stimulated phase transition to superionic state of the crystal TlSe

© R.M. Sardarly¹, N.A. Alieva¹, F.T. Salmanov¹, S.M. Gakhramanova¹,
R.N. Mekhdieva¹, R.S. Agaeva²

¹Institute of Radiation Problems of the National Academy of Sciences of Azerbaijan,
AZ1143 Baku, Azerbaijan

²Mingechaur State University,
Mingechaur, Azerbaijan

E-mail: sardarli@yahoo.com

Received July 8, 2022

Revised July 8, 2022

Accepted July 27, 2022

The temperature-frequency dependences of: electrical conductivity ($\sigma(\mu, T)$), the real and imaginary parts of the complex permittivity ($\epsilon'(\nu, T)$) and ($\epsilon''(\nu, T)$), the complex impedance of the TlSe compound when exposed to various doses of gamma radiation. The process of the occurrence of concentration polarization at the boundary of the ion conductor blocking contact is investigated. The temperature-frequency-dose interval of the occurrence of ionic conductivity and the Warburg impedance has been established and a radiationally stimulated phase transition to the superionic state of the TlSe crystal has been detected.

Keywords: complex impedance, blocking contact, of ionic conductivity.

DOI: 10.21883/PSS.2022.12.54379.428

1. Introduction

The effect of radiation on solids leads to a change in their structural and phase states and physical properties. Radiation-stimulated methods of material processing are based on controlled changes in electrophysical properties by creating structural defects in them that change the energy spectrum of the material and create new phases. Currently, the focus is on the physical nature of radiation-stimulated modifications of the properties of compounds and the creation of new structures.

The development of modern materials for the creation of ionists, ion conductors, mini-accumulators, fuel cells and other devices whose operation is based on the characteristics of the conductivity of solid electrolytes (superionic conductors) depends on the search for new compounds that have the appropriate electronic and phonon spectrum, as well as the appropriate structure.

The characteristic features of superionic crystals are: the presence of mobile ions in the crystal, which should be more than the corresponding crystallographic positions; weak energy of the disordering of ions by positions; the existence of a connected grid of conduction channels.

The TlSe compound crystallizes in a volume-centered chain structure, symmetry D_{4h}^{18} ($I4/mcm$). A distinctive feature of this structure is the presence of thallium atoms in two different valence states Tl^+ and Tl^{3+} and, respectively, in two different crystallographic positions, the ions Tl^{3+} and their nearest tetrahedral environment, which consists of four Se^{2-} ions, form negatively charged chains $Se_2^{2-}-Tl^{3+}-Se_2^{2-}$ directed along the tetragonal axis. The monovalent ions Tl^+

are located between four chains and at the same time have an octahedral environment of eight ions Se^{2-} [1]. Fragments of these chains are interconnected by Tl^{+1} ions, so the compound formula can be expressed as $Tl^+[Tl^{3+}Se_2^{2-}]$. The chains are interconnected by a weak Van der Waals bond with ions Tl^{+1} (Fig. 1).

This paper presents the results of studies of the temperature-frequency dependence of the ionic conductivity and the impedance of the TlSe crystal when exposed to various doses of γ -radiation.

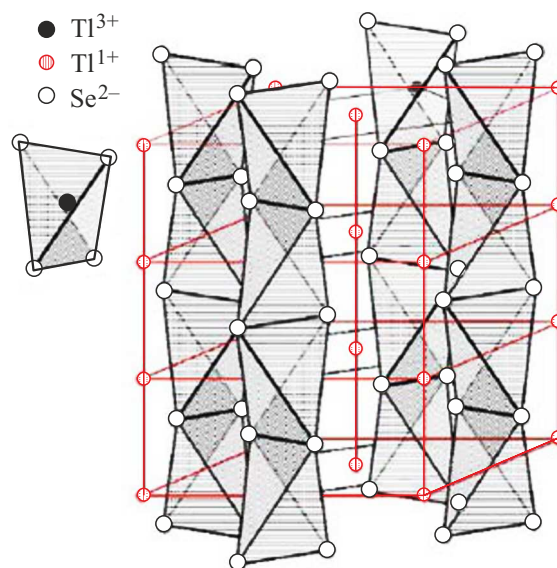


Figure 1. Crystal structure TlSe.

2. Experimental procedure

The synthesis of the TlSe compound was carried out by direct fusion of high-purity initial components in evacuated ($\sim 10^{-2}$ Pa), and sealed quartz ampoules. Single crystals were grown by the vertical Bridgman method. In the synthesis, high-purity elementary components manufactured by Evochem Advanced Materials GMBH were used (purity not less than 99.99). Taking into account the high vapor pressure of selenium at the melting point, the synthesis of the compound was carried out in a two-zone mode. After synthesis, the sample was annealed at a temperature of 400 K. The synthesized samples were identified by differential scanning calorimetry (DSC) and X-ray phase analysis (XPA).

Single crystals were grown by the vertical Bridgman method. To measure the temperature dependences of the permittivity and electrical conductivity of TlSe materials, capacitors were manufactured in which plates of the materials under study served as a dielectric. The capacitor plates were obtained by applying a silver conductive paste on the surface of the plates. Studies of the complex dielectric permittivity ($\epsilon^* = \epsilon' + \epsilon''$) and electrical conductivity were carried out with a digital impedance meter E7-25 at frequencies 20–10⁶ Hz in the temperature range 100–450 K. The amplitude of the measuring field did not exceed 1 V · cm⁻¹.

3. Results and discussion

3.1. Temperature dependence of conductivity

Figure 2 shows the temperature dependence of the electrical conductivity for a TlSe crystal of irradiated γ -quanta.

The insert to the figure shows the same dependence in coordinates $\ln(\sigma T)$ from $1000/T$. The measurements were performed at γ -irradiation doses of 0; 0.25 and 0.75 mGy. As can be seen from the figure, with an increase in the radiation dose, the curves (1, 2 and 3) there is a sharp increase in conductivity with an increase in the radiation dose. As can be seen from the insert to the figure, the experimental points of temperature dependence $\ln(\sigma T)$ from $1000/T$ in the area of a sharp jump in electrical conductivity fit well on a straight line, which for the case of ionic conductivity is described by the equation [2,3]:

$$\sigma T = \sigma_0 \exp(-\Delta E/kT).$$

Here ΔE — conduction activation energy, k — Boltzmann constant. The observed sharp increase in electrical conductivity in the TlSe crystal, with an increase in the radiation dose, can be explained by a sharp increase in energy equivalent crystallographic positions caused by radiation defects. At the same time, the placement of mobile ions in the crystal becomes larger than the crystallographic octahedral positions occupied by Tl^{+1} before radiation exposure. The crystallographic structure of the TlSe compound consists of anionic chains formed by TlSe_4 tetrahedra (Fig. 1).

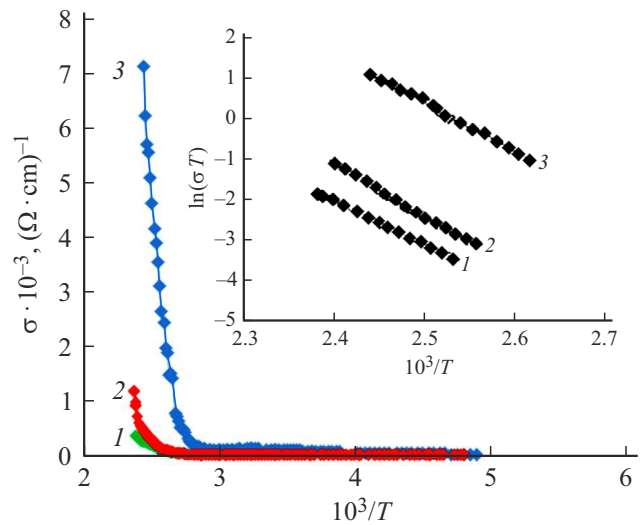


Figure 2. Temperature dependence of the TlSe crystal conductivity of irradiated γ -quanta. The insert shows the same dependence in coordinates $\ln(\sigma T)$ from $1000/T$. The numbers 1, 2 and 3 show the doses of γ -irradiation, 0, 0.25 and 0.75 mGy, respectively.

The ions Tl^{+1} are located in octahedral voids between the chains TlSe_4 . From crystal chemical considerations, it follows that the chain structure of TlSe crystals and the position of Tl^{+1} ions most contribute to the mobility of thallium ions.

The insert to Fig. 2 shows the dependence of $\ln(\sigma T)$ on $1/T$, at temperatures above the conductivity jump for samples exposed to radiation doses: 0 (initial); 0.25 and 0.75 mGy of TlSe crystals. There is an increase in conductivity with an increase in the absorbed dose. The presence of a TlSe crystal chain structure, as well as the existence of Tl^{+1} ions in octahedral voids, which are connected by a weak Van der Waals bond with chains formed by TlSe_4 tetrahedra, form conduction channels for Tl^{+1} ions.

3.2. Frequency dependence of conductivity

At low frequencies ($\nu < 10^6$ Gz), the conductivity over delocalized states does not experience frequency dispersion. At these frequencies, the real part of the conductivity is determined by the phonon mechanism, and with increasing frequency, phononless conductivity begins to prevail over relaxation conductivity. The power dependence indicates that charge transfer occurs due to carrier jumps. This behavior of the frequency dependence of the conductivity is characteristic of carrier jumps over localized states. At low frequencies, the frequency dependence of the real part of the conductivity is close to the linear $s \sim 1$. Thus, the solution of the problem associated with the determination of a specific charge transfer mechanism is associated with structural features, namely, the nature of disorder. The results of studies of the frequency dependence of the conductivity of TlSe crystals at $T = 300, 350$ and 400 K and

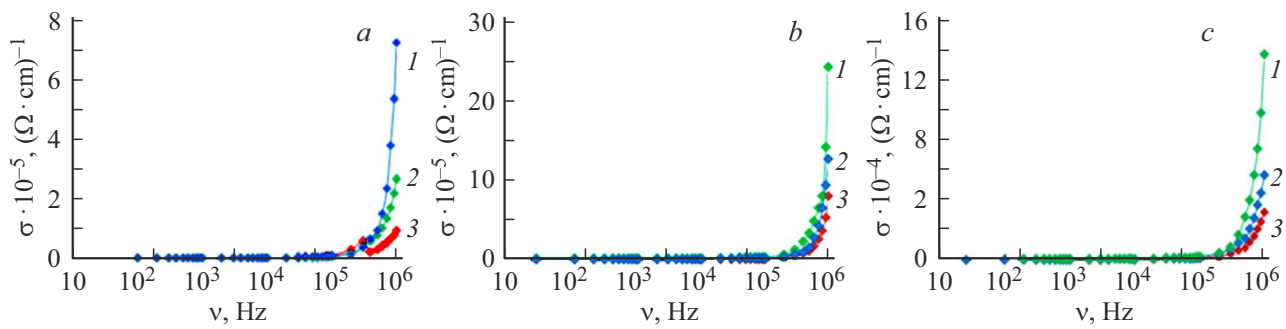


Figure 3. Frequency dependence of the electrical conductivity of the TlSe crystal. The measurements were performed at temperatures: 1 — 300, 2 — 350 and 3 — 400 K, and at doses of γ -irradiation: *a* — 0; *b* — 0.25; *c* — 0.75 MGy.

doses of γ -irradiation of 0, 0.25 and 0.75 mGy are presented in Fig. 2.

As can be seen from the figures, the curves $\sigma(\lg \nu)$ constructed for non-irradiated TlSe crystal samples (curves, *a* in Fig. 3), can be divided into two sections: measurements performed at low temperatures (300 and 350 K) and low frequencies $< 10^3$ Hz. Under these experimental conditions, a weak frequency dependence of the conductivity is observed. A significant variance is observed when measuring at frequencies above $> 10^3$ Hz. At the same temperatures and in the same frequency range, TlSe crystal samples irradiated with γ -quanta with a dose of 0.25 mGy, have a weak frequency dependence (curves *b* in Fig. 3). This behavior of the dependence $\sigma(\lg \nu)$ when irradiated with a dose of 0.25 mGy quanta may be associated with radiation annealing of samples, leading to „healing“ of the initial, uncontrolled defects in the TlSe crystal.

Measurements carried out at a temperature of 400 K on samples irradiated with γ -quanta at a dose of 0.75 mGy (curves *c* in Fig. 3), show a significant increase in conductivity and dispersion. This behavior of the conductivity of TlSe crystals may be associated with an increase in the ionic component of the conductivity, that is, at an irradiation dose of 0.75 mGy and a temperature of 400 K, a phase transition of the crystal to the superionic state occurs. A characteristic feature of the studied dependence $\sigma_{AC} \sim (f)$ is that at low frequencies it is expressed as $\sigma_{AC} \sim f^{0.6}$, and in the frequency range $f \sim 5 \cdot 10^5$ Hz this dependence turns out to be equal to $\sigma_{AC} \sim f^{0.8}$. Such frequency dependence, according to [4], characterizes the conductivity by localized states near the Fermi level.

3.3. Impedance

The methods of impedance spectroscopy are used in the study of electrophysical processes occurring at the interface of the electrode ion-conducting material, dielectric and transport properties of materials, the establishment of the mechanism of electrochemical reactions, the study of the properties of porous electrodes. We have measured the real and imaginary parts of the impedance of TlSe compound samples at temperatures of 300, 350 and 400 K and doses

of γ -irradiation of 0; 0.25 and 0.75 mGy. The obtained data are presented in the form of an impedance hodograph on the complex plane (Fig. 4). Measurements are made in the frequency range 20– 10^6 Hz.

Fig. 4, *a* (*I*) shows the dependence $Z''(Z')$ obtained at 300 K and 0 mGy, as can be seen from the figure, the dependence is a straight line. This dependence indicates that at these values of temperature and the absence of radiation exposure, the ion transfer has not yet begun, i.e., the phase transition to the superionic state has not yet occurred. The curve obtained at room temperature, and after radiation exposure with a 0.25 mGy nozzle, is shown in Fig. 4, *b* (*I*). On Fig. 4, *c* (*I*) the dependence hodograph $Z''(Z')$ is presented measured at 300 K and an irradiation dose of 0.75 mGy. As can be seen from these figures (*a* (*I*), *b* (*I*) and *c* (*I*)), the curve of the impedance hodograph of the TlSe crystal, with an increase in the radiation dose, is deformed from the linear dependence (Fig. 4, *a* (*I*)), up to the semicircle (fig. 4, *c* (*I*)), the centers of which are located on the real axis, while the charge transfer process is characterized by one relaxation time. The dependence shown in Fig. 4, *c* (*I*), is a hodograph corresponding to a homogeneous sample with a low-resistance and non-blocking contact. The results obtained may indicate that TlSe crystals, at room temperature, and when irradiated with γ - rays at a dose of 0.75 mGy experiences a radiation-stimulated phase transition to a superionic state.

Frequency values (f_{\max}) corresponding to the maximum of $Z''(Z')$ and their relaxation times (τ), frequencies corresponding to the beginning of dispersion (f_{jamp}), for TlSe crystal samples at 300; 350 and 400 K and doses of γ -irradiation: 0; 0.25; 0.75 Mgy (table).

As can be seen from the table and Fig. 4, the imaginary parts of the impedance detect a maximum at frequencies f_{\max} corresponding to the condition $C_{\text{eff}}R_{\text{eff}}\omega_{\max} = 1$, where C_{eff} and R_{eff} — effective parameters of the equivalent circuit, $\omega_{\max} = 2\pi f_{\max}$ — circular frequency. On unirradiated samples Fig. 4 (*a* (*I*); *b* (*I*); *c* (*I*)), with increasing temperature, the frequency f_{\max} increases, corresponding to the maximum Z'' . As it can be seen from Fig. 4, *a* (*I*), dependency $Z''(Z')$ has a linear character, such a dependence

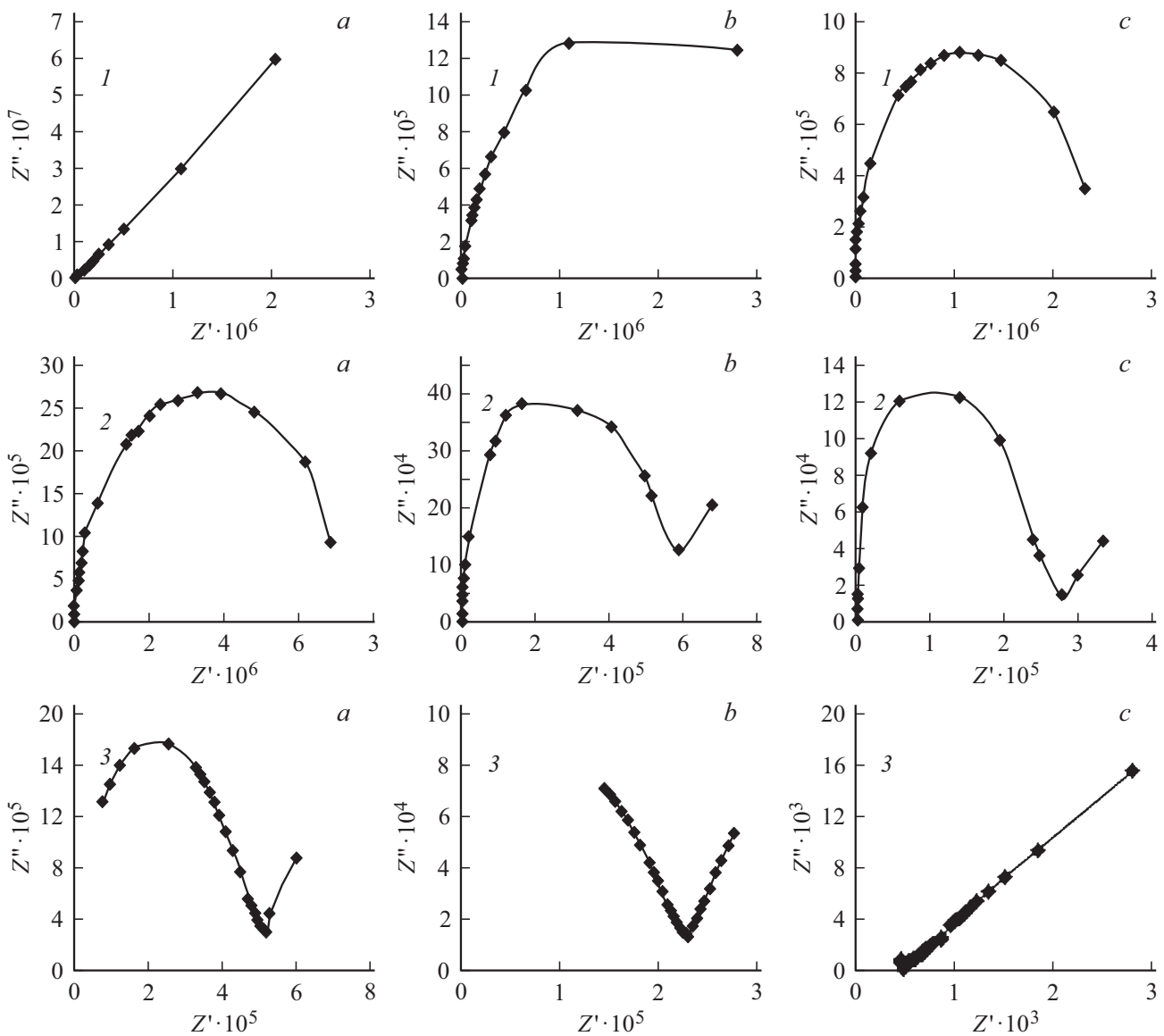


Figure 4. Impedance hodograph $Z''(Z')$ of the TiSe crystal. The measurements were performed at temperatures: 1 — 300; 2 — 350 and 3 — 400 K, and at doses of γ -irradiation: a (1, 2, 3) — 0; b (1, 2, 3) — 0.25; c (1, 2, 3) — 0.75 MGy.

of conductivity is characteristic of phononless (resonant) hopping conductivity of localized charge carriers.

The curves shown in Fig. 2, a, b, c — are curves measured at 350 K, and received radiation doses: — 0; b — 0.25; c — 0.75 mGy. As can be seen from Fig. 2, a, at a temperature of 350 K on non-irradiated TiSe crystal samples, a hodograph arc is visible on the complex plane, which indicates that the crystal has passed into a state with ionic conductivity. A further increase in the absorbed dose (b — 0.25; c — 0.75 mGy) leads to the appearance of „rays“ in the low-frequency area of the hodograph. Thus, the observed rays at a temperature of 350 K and doses of b — 0.25; c — 0.75 mGy indicate additional contributions to conductivity, which, apparently, is associated with diffuse ion transport Tl^{1+} there is an ion conductor and electrode in the interface.

The occurrence of „rays“ in the low-frequency area of the impedance hodograph of the TiSe crystal indicates the presence of a diffuse Warburg impedance [5]. On Fig. 4 curves 3 reflect the results of measurements of the TiSe crystal impedance at 400 K and at radiation doses of 0, 0.25 and 0.75 mGy, respectively, curves 3 (a, b, c). As can be seen from Fig. 3, a, an arc is visible on the impedance hodograph at 400 K, as well as a „beam“, which we associate with diffuse ion transfer in the near-contact area of the TiSe crystal (ion conductor) — electrode (Ag). With a further increase in the irradiated dose, the curves 3 (b and c) in Fig. 4 the arc of the impedance hodograph is shifted to the high-frequency area. In this case, the beam, on the impedance curve, also shifts to the high frequency area. When irradiated with a dose of 0.75 mGy, the hodograph arc continues to shift to the

Frequency values (f_{\max}) corresponding to the maximum of Z'' (Z'), and their relaxation times (τ), frequencies corresponding to the beginning of the variance (f_{jamp}), for crystal samples TlSe at 300; 350 and 400 K and doses γ -irradiation: 0; 0.25; 0.75 Mgy

TlSe	T (K)	f_{\max} (kHz)	$\tau = 1/2\pi f_{\max}$	f_{jamp} (kHz)
0 MGy	300	–	–	2
	350	0.4	$3.9 \cdot 10^{-4}$	20
	400	30	$5.3 \cdot 10^{-6}$	60
0.25 MGy	300	0.1	$1.5 \cdot 10^{-3}$	4
	350	0.6	$2.6 \cdot 10^{-4}$	30
	400	60	$2.65 \cdot 10^{-6}$	–
0.75 MGy	300	1	$1.5 \cdot 10^{-4}$	50
	350	3	$5.3 \cdot 10^{-5}$	80
	400	–	–	–

high frequency area (curve 3(c)) and its measurement is beyond our experimental capabilities. At the same time, in Fig. 3, c, the previously observed „beam“ remains in the low-frequency area of the hodograph, which we associate with the polarization capacitance and resistance of the near-electrode area. That is, the impedance hodograph shown in Fig. 4, 3(c) simulates the linear diffusion impedance, known as the diffuse Warburg impedance [5–8].

As can be seen from the curves of the impedance hodographs of the TlSe crystal shown in Fig. 4, „rays“ in the low-frequency area of the diagrams arise both with an increase in temperature and with an increase in the irradiated dose. It is known [6] that the processes occurring at the interface of various conductive materials are described within the framework of the frequency response model, which is associated with the presence of polarization resistance in the near-electrode area, and the polarization capacitance associated with the accumulation of charge in the area of the double electric layer.

4. Conclusion

Temperature-frequency studies of the conductivity and impedance of a TlSe crystal subjected to various doses of γ -irradiation (0, 0.25 and 0.75 mGy) allowed us to establish a radiation-stimulating effect on the nature of charge transfer in the crystal under study. It is shown that as a result of the influence of γ -quanta, the nature of conductivity changes in the volume of the crystal. In samples not exposed to radiation, charge transfer is carried out by electrons, radiation exposure leads to the fact that the conductivity becomes predominantly ionic (superionic). In addition, it is shown that γ -irradiation strongly affects ion-polarization processes occurring in the near-contact area, which leads to

the appearance of a diffuse Warburg impedance caused by γ -irradiation.

Conflict of interest

The authors declare that they have no conflict of interest

References

- [1] A.M. Panich, R.M. Sardarly. Physical Properties of the Low Dimensional A_3B_6 and $A_3B_3C_2^6$ Compounds. Nova Science Publishers, N.Y. (2010).
- [2] A.S. Nowick, A.V. Vaysleyb, I. Kuskovsky. Phys. Rev. B **58**, 8398 (1998).
- [3] Yu.Ya. Gurevich, Yu.I. Harkats. Osobennosti termodinamiki superionnykh provodnikov. UFN, **136**, 4, 693 (1982). (in Russian).
- [4] N. Mott, E. Davis. Electronic processes in non-crystalline substances. Mir, M. (1982).
- [5] R.M. Sardarly, A.P. Abdullaev, N.A. Aliyeva, F.T. Salmanov, M.Yu. Yusifov, A.A. Orudzheva. FTP, **52**, 1111 (2018). (in Russian).
- [6] J.R. Macdonald. Impedance Spectroscopy. John Wiley & Sons, Inc., New Jersey (2005). 595 p.
- [7] R.M. Sardarly, N.A. Aliyeva, F.T. Salmanov, R.M. Abbasova. Mod. Phys. Lett. B **34**, 5, 2050113-1-2050113-12 (2020).
- [8] R.M. Sardarly, N.A. Aliyeva, F.T. Salmanov, R.N. Mehdiyeva, S.M. Gakhramanova. Mod. Phys. Lett. B **35**, 33, 2150504-1-2150504-9 (2021).